

Comments on the Conceptual Design Report of CBM detector magnet (Version of Feb 2018)

P.Fabbricatore, S.Farinon Genova March 9th 2018

The design of CBM magnet has been improved in many parts. Here we only underline some critical areas we still see.

- **Struts.** The design of the struts has been deeply modified. Also this structure is designed for compressive load. As in previous we ask if all faulty scenarios have been considered leading to a possible tensile load on the struts and possible effects.
- **Coil.** The superconducting coil lay-out has been modified introducing a copper case (U-shaped) used as bobbin during the winding and remaining as a permanent component. Considering that at the same time the coil is now indirectly cooled, the copper case helps in cooling homogeneously the winding. However there are some drawbacks to be considered. 1) Coil delamination. The copper contracts more than the coil; this fact coupled with the radial dilatation due to energization could cause a delamination of the coil from the copper case. According our personal experience, for past magnets this effect caused a long training and, in worst case, the magnet cannot get its nominal current. In order to prevent this occurrence one should make precise mechanical analysis (2D should be enough) considering also the beneficial effect of the winding tension. Secondly the construction should be carefully monitored to be sure that the radial pre-stress of the winding is at such level to prevent coil detaching from the copper case. Finally the thermal contraction on the coil should be very well known for allowing an accurate design. 2) Eddy currents. During field ramp and during quench eddy currents are induced in the copper case. From one side this effect helps in uniformly quench the whole coils during a fast dump (quench back), but at the same time it could limit the field ramp due to the heating of the case. The presence of the copper case should be included in the circuit scheme (as the one shown in Fig.39). Due to the large induced currents, the mechanics of the magnet could be affected during the quench. May be there is no major problem, but this effect shall be analysed.
- **Coil Cooling.** In the present design the coils are indirectly cooled. Considering the thickness of the ground insulation (limiting the cooling with a LHe bath), we think that this solution is acceptable provided that the heat loads are correctly evaluated with suitable margins. One crucial point is related to the thermal intercepts of the struts. It would be very useful to make an experimental test on a single strut for checking the heat load to 4.2K. Alternatively a 3D thermal analysis of the temperature distribution in the coil with all heat loads included (with a very large margin) could be done. Finally there is a general consideration to be done: this solution with indirect cooling is different from the one used in the Samurai magnet, which could have been

considered a benchmark for the CBM magnet. Nothing bad in this choice, but it should be clear that Samurai magnet cannot be longer considered a reference for CBM magnet design.

- **Material properties.** The data shown in Table 5, should be re-checked specially regarding the thermal expansion coefficient, which looks 10% higher than the real one. The Young modulus seems the one at room temperature (lower than at 4.2K).
- **Heat load.** As reported in a previous review of us, the heat loads to 4.5 K appear optimistic. We are repeating here that these heat loads have been computed with too simplified assumptions and sometime optimistic values were considered (too low emissivities).

Electromagnetic finite element analysis of CBM magnet

The electromagnetic analysis presented in the CDR is not fully satisfactory as it calculates the fields by a Mermaid 3D analysis and the forces by an ANSYS 2 D analysis. This section reports the electromagnetic 3D analysis we performed on the CBM magnet using the finite element code ANSYS Apdl 18.2. Fig. A and B show the model and the finite element mesh in full and half view, even if, for symmetry reasons, only 1/8 of the system is enough to fully describe the magnetic field distribution. Main dimensions are taken from the Conceptual Design Report, Feb. 2018.

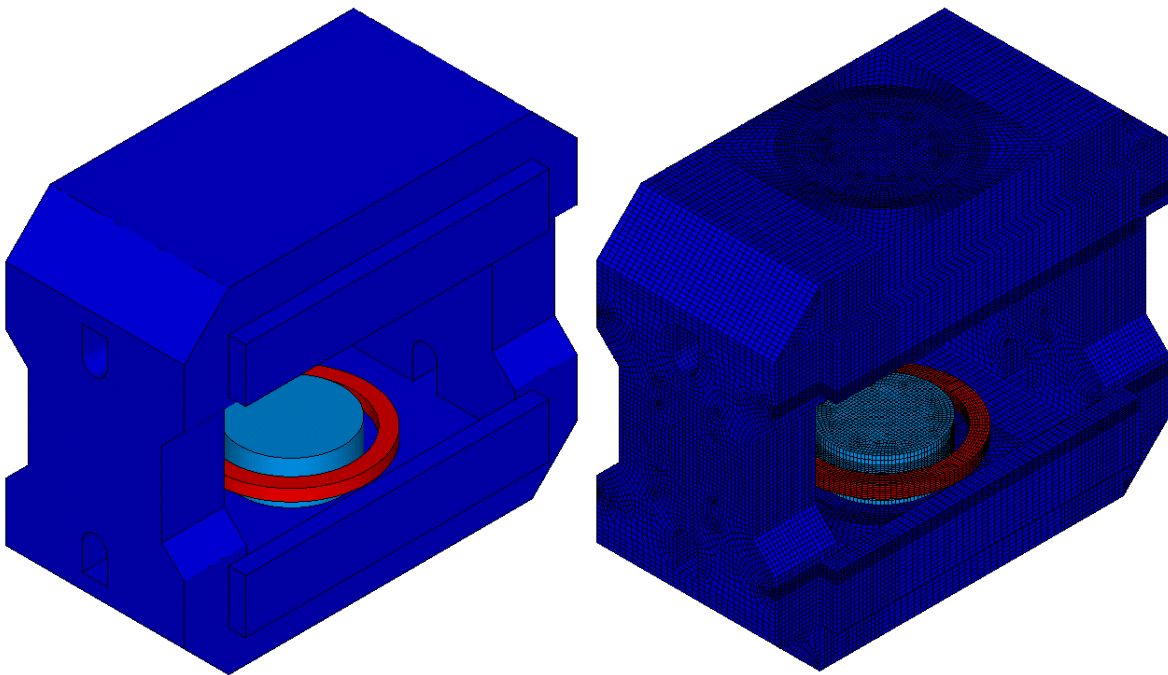


FIG.A: Model (left) and mesh (right) of the finite element model of CBM magnet (full view).

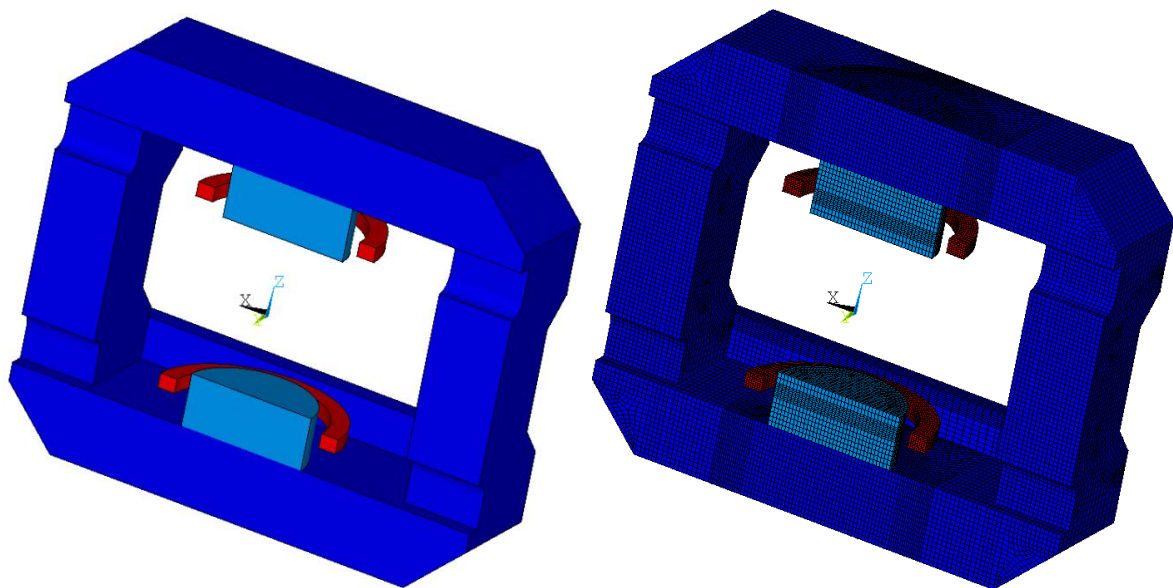


FIG.B: Model (left) and mesh (right) of the finite element model of CBM magnet (half view).

The complete model, including air, is shown in Fig. C in 1/8 symmetry. It has around 600.000 nodes and 600.000 elements. A cubic box of air, 4.4 m in half side, surrounds the magnet system. Boundaries are represented via infinite elements (the outer box in Fig. C right), which allow modeling an open boundary of an unbounded field problem.

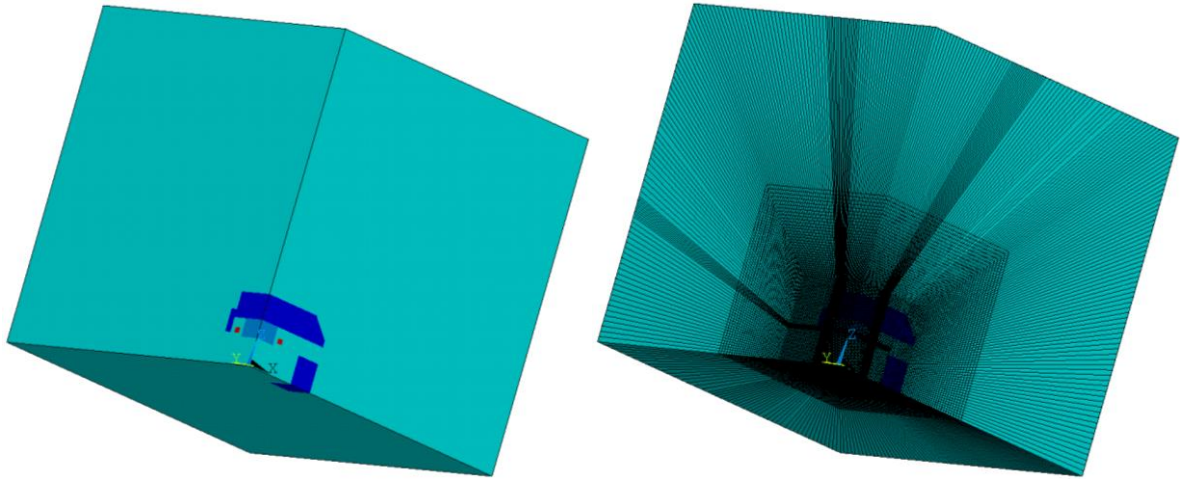


FIG.C: Complete model (left) and mesh (right) of the finite element model of CBM magnet (1/8 view).

Two different nonlinear properties have been defined: the steel of the pole (Armco) and the steel of the iron yoke (Steel 1010). Properties in Tab.3 of CDR (page 17) have been converted into BH curves, as required by ANSYS. It emerged that ANSYS suffers the atypical nonlinear behavior of the first 12 data points, which has been rectified (see Fig. D right). Also, the curves have been prolonged beyond 2.5 T, as the peak field in iron is larger than 4 T. The two adopted BH curves are plot in Fig.D and described in Tab.I.

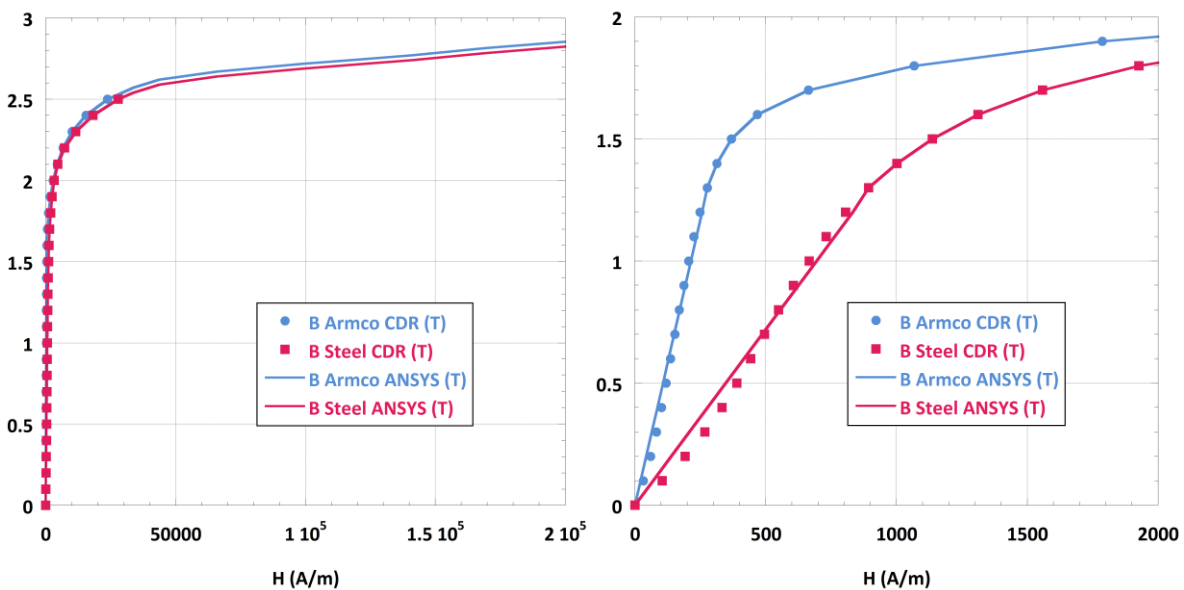


FIG.D: BH curves as extracted from CDR (dots) and elaborated for ANSYS (lines).

TAB.I: BH curves of Armco (poles) and Steel 1010 (yoke).

Armco		Steel 1010	
B (T)	H (A/m)	B (T)	H (A/m)
0.0000	0.0000	0.0000	0.0000
0.10000	21.402	0.10000	69.444
0.20000	42.804	0.20000	138.89
0.30000	64.205	0.30000	208.33
0.40000	85.607	0.40000	277.78
0.50000	107.01	0.50000	347.22
0.60000	128.41	0.60000	416.67
0.70000	149.81	0.70000	486.11
0.80000	171.21	0.80000	555.56
0.90000	192.62	0.90000	625.00
1.0000	214.02	1.0000	694.44
1.1000	235.42	1.1000	763.89
1.2000	256.82	1.2000	833.33
1.3000	276.92	1.3000	893.42
1.4000	313.25	1.4000	1001.6
1.5000	368.49	1.5000	1137.0
1.6000	467.70	1.6000	1311.6
1.7000	663.71	1.7000	1558.4
1.8000	1067.6	1.8000	1926.8
1.9000	1787.1	1.9000	2479.4
2.0000	2886.5	2.0000	3308.4
2.1000	4464.1	2.1000	4731.0
2.2000	6715.7	2.2000	7314.2
2.3000	10136	2.3000	11625
2.4000	15546	2.4000	18256
2.5000	23835	2.5000	27919
2.5200	26750	2.5400	33760
2.5700	33760	2.5900	43800
2.6200	43800	2.6400	66000
2.6700	66000	2.6890	99740
2.7190	99740	2.7150	1.2096e+05
2.7450	1.2096e+05	2.7400	1.4121e+05
2.7700	1.4121e+05	2.7843	1.6960e+05
2.8143	1.6960e+05	2.8396	2.1217e+05
2.8696	2.1217e+05	2.9305	2.8313e+05
2.9605	2.8313e+05	3.0027	3.3989e+05
3.0327	3.3989e+05	3.1106	4.2504e+05
3.1406	4.2504e+05	3.2898	5.6695e+05
3.3198	5.6695e+05	3.6474	8.5076e+05
3.6774	8.5076e+05	4.7182	1.7023e+06
4.7482	1.7023e+06	5.2534	2.1280e+06
5.2834	2.1280e+06		

The current density in the winding is $1749\text{-}686/131/160=57.243\text{ MA/m}^2$. The resulting magnetic field in the winding is shown in Fig. E. The **peak field, 3.66 T**, is lower than predicted in the CDR, 3.89 T.

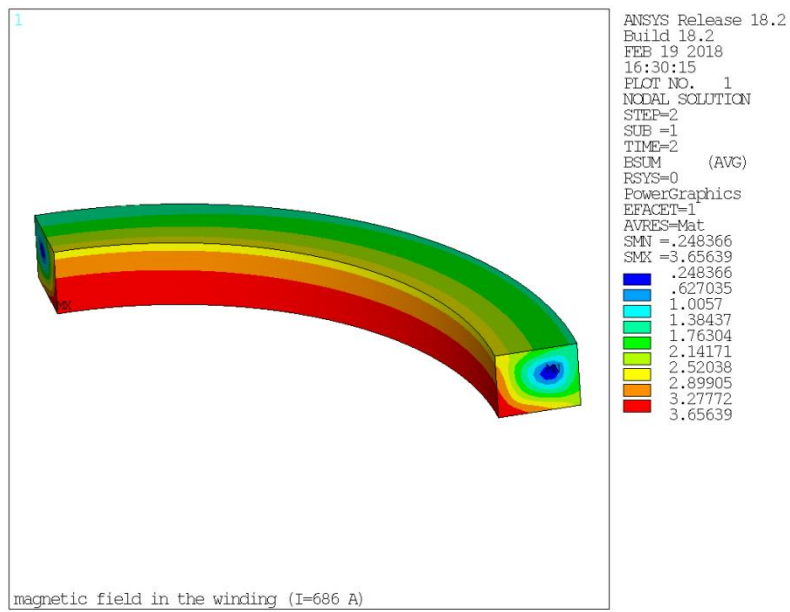


FIG.E: Magnetic field (T) in the winding.

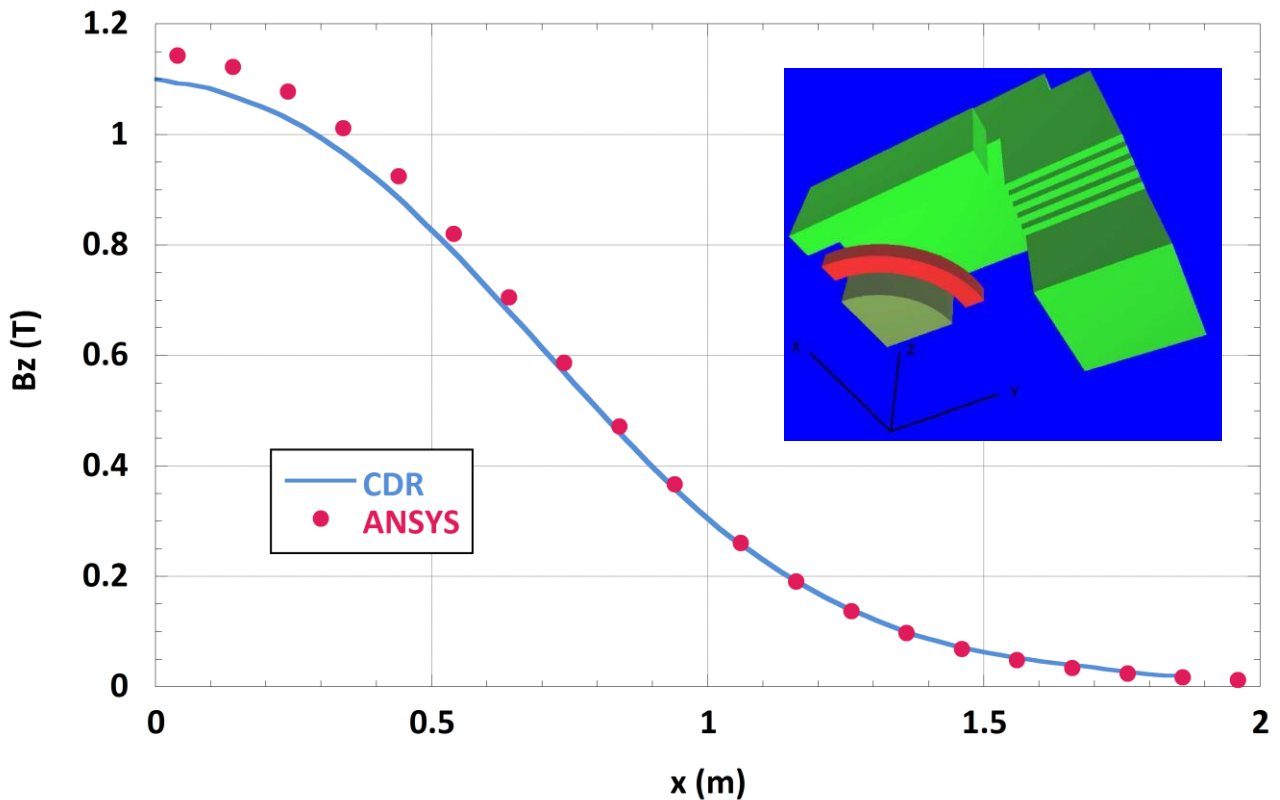


FIG.F: Bz (T) along x-axis as digitized from CDR (Fig.17) and calculated by ANSYS.

Fig. F shows the behavior of B_z along x-axis as digitized from CDR (Fig.17, page 18) and calculated by ANSYS. The maximum difference is at $x=0$, where $B_{z_{ANSYS}}=1.145$ T and $B_{z_{CDR}}=1.1$ T (~4%). The integrals along this line are $\int_{-0.5}^{0.5} B_{z_{ANSYS}} dx=1.05$ Tm and $\int_{-0.5}^{0.5} B_{z_{CDR}} dx=1.003$ Tm, with a difference of ~5%.

The magnetic field values shown in Tab. 4 of CDR (page 18) as calculated by ANSYS are listed in Tab. II, in the hypothesis they belong to the $Y=0$ plane. The agreement is fairly good, around 10%, in the region of interest, identified by the grey shadows. Instead, there is a large discrepancy in the region $110 \leq X \leq 120$, $100 \leq Z \leq 140$. Considering that the $X=110$ cm line falls within iron (at least for $100 \leq Z \leq 140$) whilst the $X=120$ cm line is surrounded by air, a corresponding significant difference in magnetic fields is expected. This difference is found in the ANSYS results but not in the CDR Tab. 4. Could you explain this discrepancy?

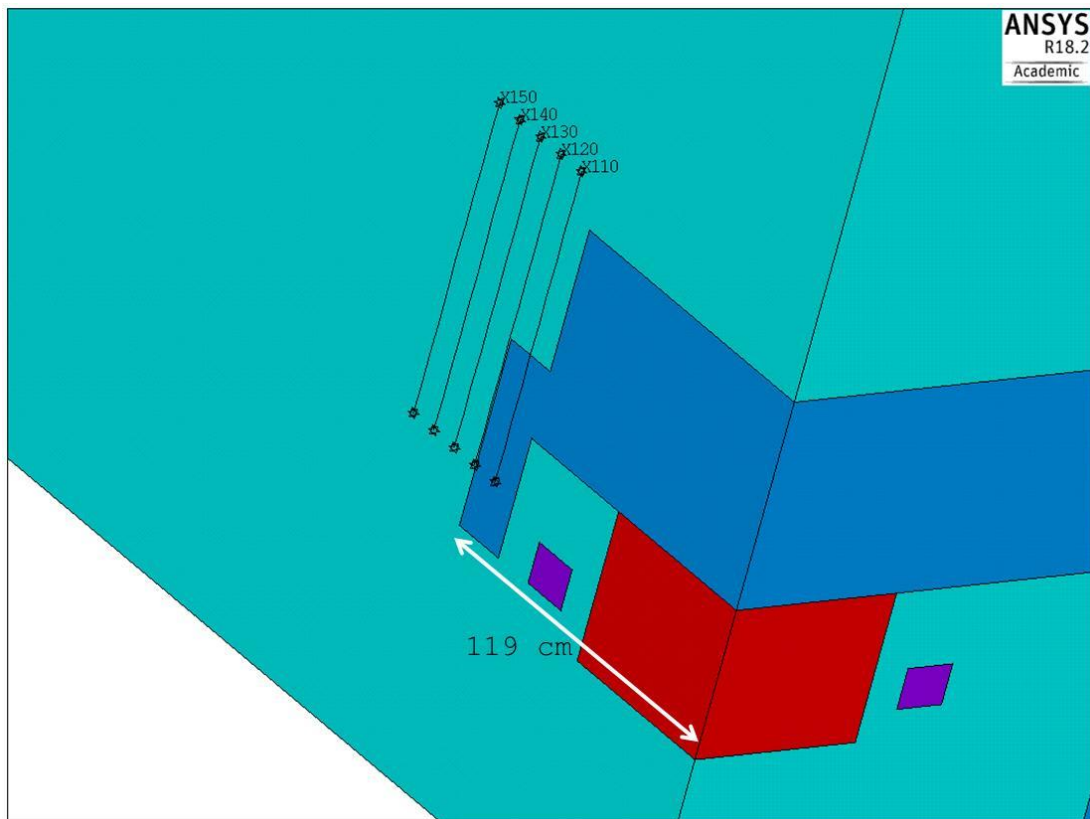


FIG.G: Position in the FE model of the grid points in Tab II.

TAB.II: Magnetic field around the RICH detector.

Z (cm)	X (cm)	110	120	130	140	150
100		1.72	0.62	0.037	0.030	0.024
110		1.73	0.64	0.024	0.021	0.018
120		1.75	0.61	0.017	0.015	0.013
130		1.37	0.39	0.013	0.012	0.010
140		0.63	0.049	0.010	0.0090	0.0080
150		0.0044	0.0067	0.0075	0.0071	0.0064
160		0.0056	0.0059	0.0060	0.0057	0.0052
170		0.0060	0.0056	0.0052	0.0049	0.0044
180		0.0064	0.0053	0.0047	0.0042	0.0038
190		0.0061	0.0049	0.0042	0.0037	0.0033
200		0.0048	0.0042	0.0037	0.0033	0.0029

The **total stored energy of the magnet system is 5.2 MJ**, the **vertical force of one coil towards the iron yoke is 3.4 MN**, to be compared with 5.1 MJ and 2.6 MN, respectively, as written in the CDR. Also, the distribution of the vertical force is not uniform in the azimuthal direction, as shown in Fig.H. Each dots in the figure represents the axial force of a sector spanning $90/33=2.73$ deg and positioned at the polar angle of its mass center, so that the summation of all the data points gives the axial force of $\frac{1}{4}$ of winding. If the axial force in the mechanical analysis is uniformly distributed, the winding stress and displacements could be underestimated.

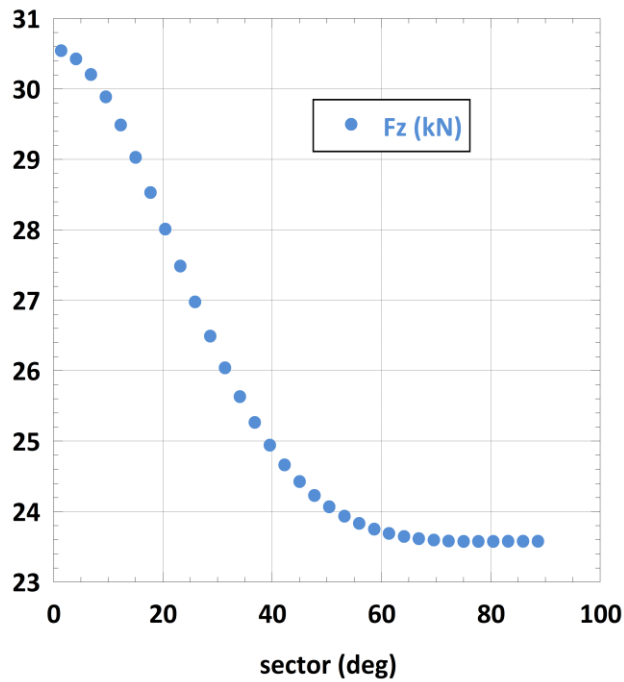


FIG.H: Azimuthal distribution of the axial component of the Lorentz force.

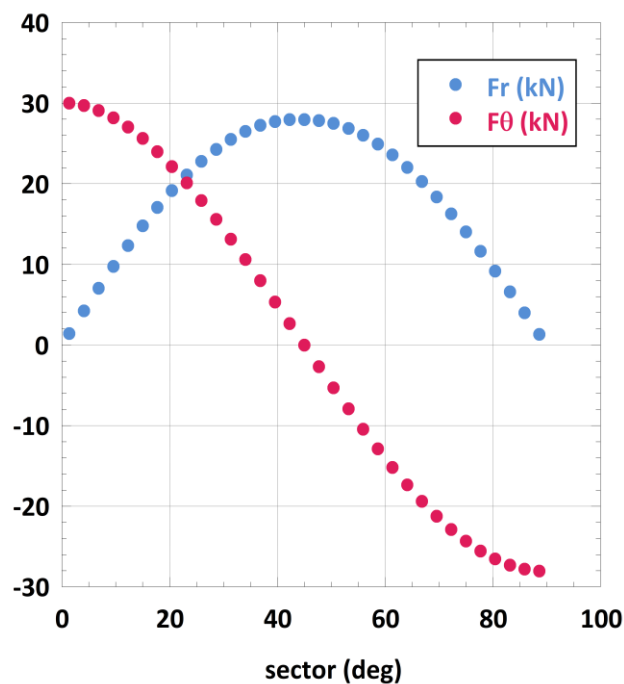


FIG.I: Azimuthal distribution of the radial and azimuthal components of the Lorentz force.

Analogously, in Fig. I the azimuthal distribution of the radial and azimuthal components of the Lorentz force is shown. The total values for each (whole) winding, are 0 for the azimuthal component and 2.4 MN for the radial component. This latter corresponds to an average magnetic pressure of 4.2 MPa, to be compared with 5 MPa evaluated in the CDR. Again in this case, the highly non uniform distribution of the radial component of the Lorentz force could result in an underestimation of stresses and displacements when its total value is applied uniformly in the whole winding.

By way of example, I made a very simple mechanical analysis, including only the winding and with the constraints shown in Fig. J. The conditions on the planes $x=0$ and $y=0$ are symmetry conditions, whilst the condition on the z displacements simulates an infinitely rigid axial support for the whole surface (no struts). On this model, I applied both the forces coming from the electromagnetic analysis and uniformly distributed radial pressure and axial loads with the same resultants. **This simple model IS NOT REPRESENTATIVE of the winding in working conditions** but it is only a model to understand the impact of the force distribution on stresses and displacements. As expected, Fig. K shows clearly that the resulting Von Mises stresses and displacements in the two cases are significantly different. Also, peak stresses and peak displacements are located in different positions and can differ by more than a factor of 2.

From CDR, it is not clear how axial force and radial pressure are applied to the winding. Our suggestion is to make a mechanical analysis using the non-homogeneous distribution Lorentz forces. We are available to supply this information in case of need. In particular, there could be a cumulative effect in the locations of the struts.

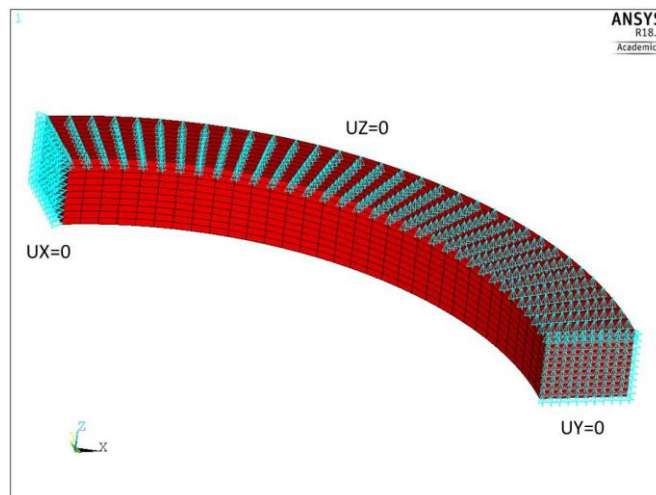


FIG.J: Simple mechanical model of CBM winding.

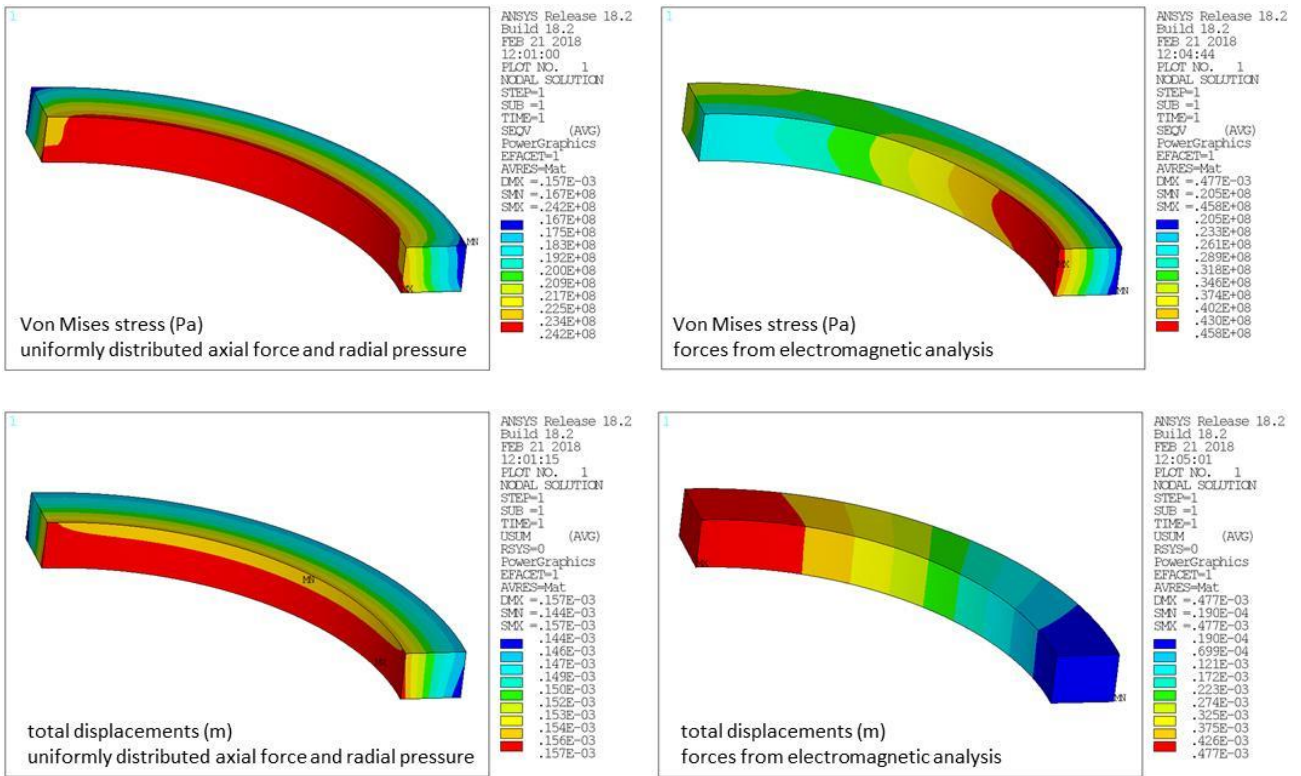
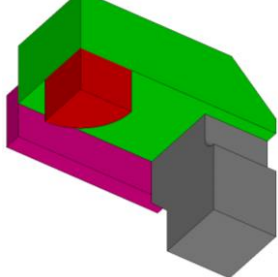
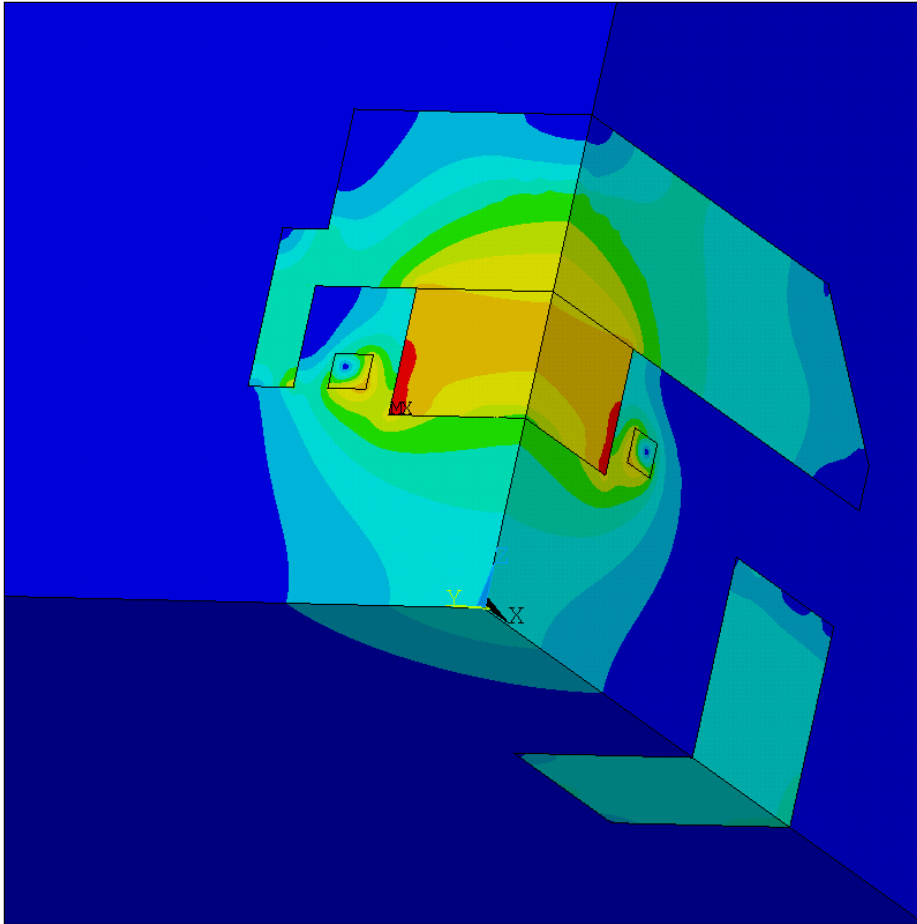


FIG.K: Von Mises stress and total displacements by uniformly distributed axial force and radial pressure (left) and with the force coming from the electromagnetic analysis (right), which include the azimuthal component.

Concerning the iron yoke, Tab. III resumes the magnetic forces on the main components. To be noticed that the axial force on the pole is 2.6 MN, to be compared with 3MN of the CDR. Including the contribution of the roof, the total axial force is 4.2 MN, so the predictions concerning the mechanical analysis of the yoke in the CDR could be underestimated.

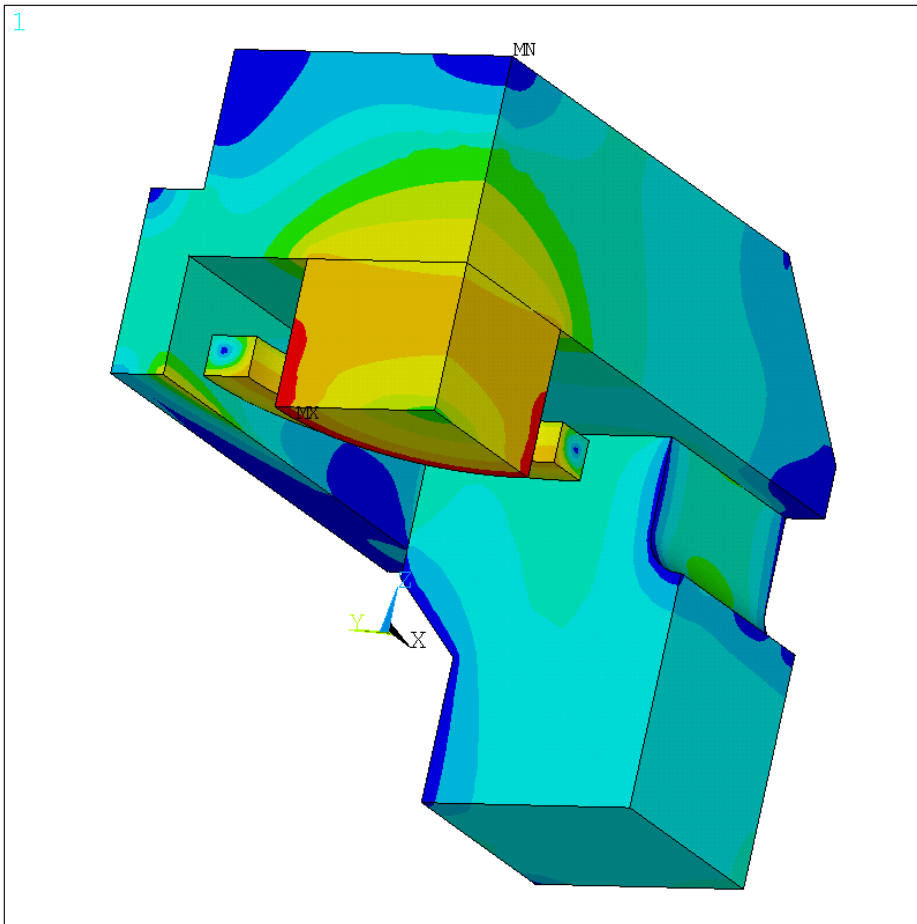
TAB.III: Magnetic forces in iron components of half magnetic system (the half which includes 1 complete pole).

	POLE (red)	ROOF (green)	PILLARS (grey)	SIDE BARS (pink)	TOTAL	
F_x (MN)	1.0	-0.4	0	-0.2	0.4	
F_y (MN)	1.0	-0.5	0	0	0.5	
F_z (MN)	-2.6	-1.4	0	-0.2	-4.2	



ANSYS Release 18.2
 Build 18.2
 FEB 20 2018
 14:42:37
 PLOT NO. 1
 NODAL SOLUTION
 STEP=2
 SUB =1
 TIME=2
 BSUM (AVG)
 RSYS=0
 PowerGraphics
 EFACET=1
 AVRES=Mat
 SMN =.146E-04
 SMX =4.3237

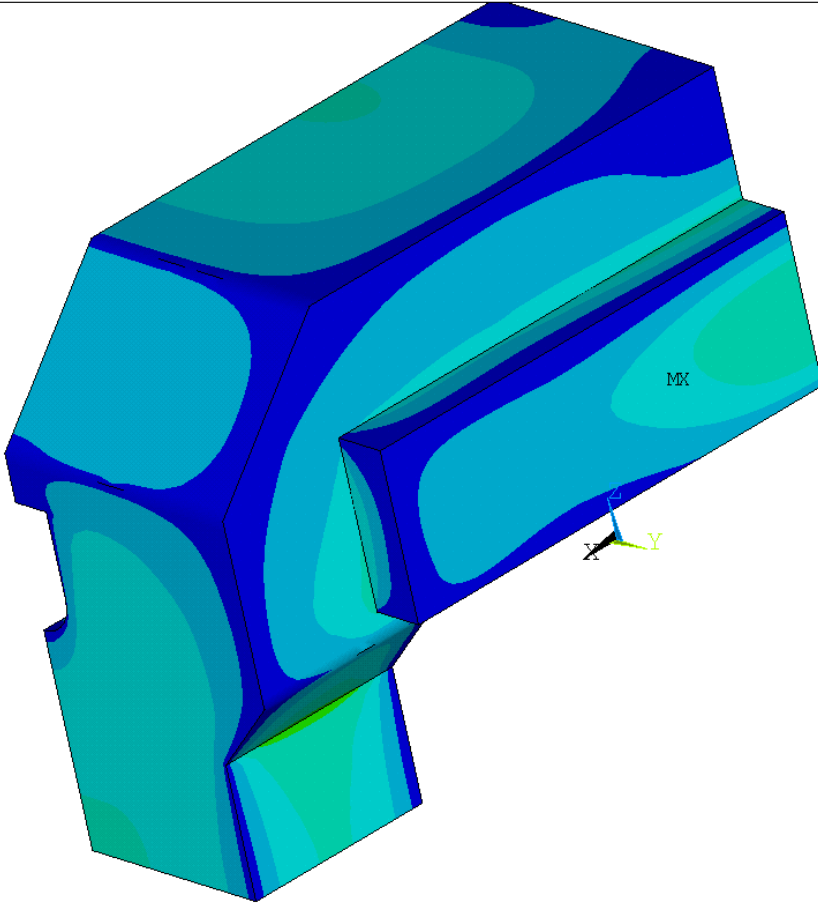
Blue	.146E-04
Light Blue	.480424
Cyan	.960833
Green	1.44124
Yellow-Green	1.92165
Yellow	2.40206
Orange	2.88247
Red-Orange	3.36288
Red	3.84329
Dark Red	4.3237



ANSYS Release 18.2
 Build 18.2
 FEB 20 2018
 14:42:58
 PLOT NO. 1
 NODAL SOLUTION
 STEP=2
 SUB =1
 TIME=2
 BSUM (AVG)
 RSYS=0
 PowerGraphics
 EFACET=1
 AVRES=Mat
 SMN =.003815
 SMX =4.3266

Blue	.003815
Light Blue	.484125
Cyan	.964435
Green	1.44474
Yellow-Green	1.92505
Yellow	2.40536
Orange	2.88567
Red-Orange	3.36598
Red	3.84629
Dark Red	4.3266

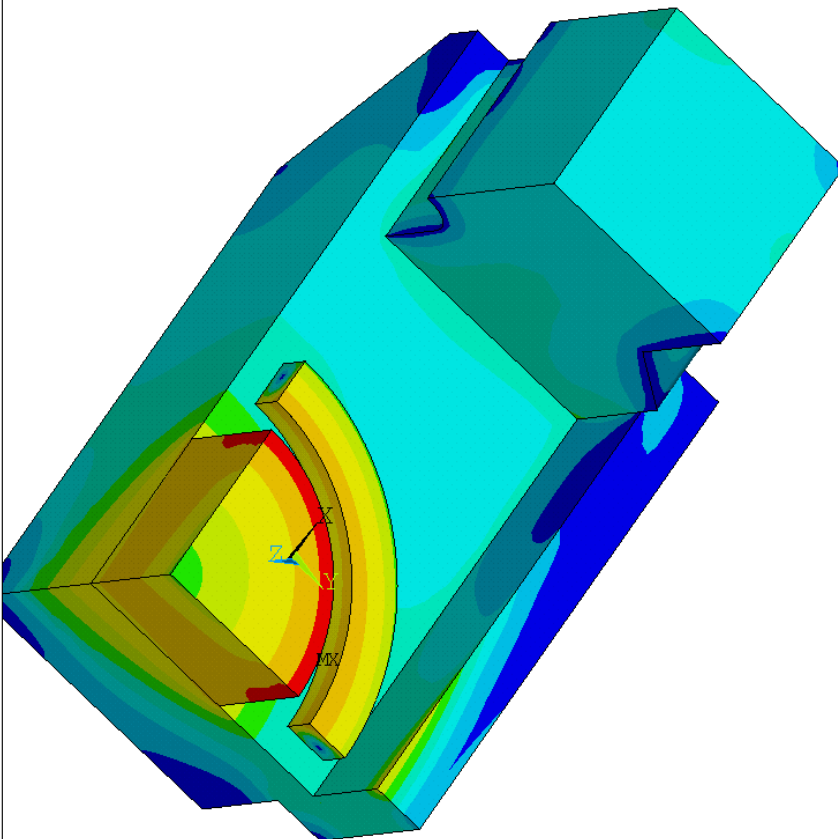
1



ANSYS Release 18.2
 Build 18.2
 FEB 20 2018
 14:43:20
 PLOT NO. 1
 NODAL SOLUTION
 STEP=2
 SUB =1
 TIME=2
 BSUM (AVG)
 RSYS=0
 PowerGraphics
 EFACET=1
 AVRES=Mat
 SMN =.003815
 SMX =4.3266

Blue	.003815
Light Blue	.484125
Cyan	.964435
Light Green	1.44474
Green	1.92505
Yellow-Green	2.40536
Yellow	2.88567
Orange	3.36598
Red-Orange	3.84629
Red	4.3266

1



ANSYS Release 18.2
 Build 18.2
 FEB 20 2018
 14:43:38
 PLOT NO. 1
 NODAL SOLUTION
 STEP=2
 SUB =1
 TIME=2
 BSUM (AVG)
 RSYS=0
 PowerGraphics
 EFACET=1
 AVRES=Mat
 SMN =.003815
 SMX =4.3266

Blue	.003815
Light Blue	.484125
Cyan	.964435
Light Green	1.44474
Green	1.92505
Yellow-Green	2.40536
Yellow	2.88567
Orange	3.36598
Red-Orange	3.84629
Red	4.3266